

Tamaz KALABEGISHVILI<sup>1,2</sup>, Ivane MURUSIDZE<sup>2</sup>, Elena KIRKESALI<sup>1,3</sup>  
Alexander RCHEULISHVILI<sup>1</sup>, Eteri GINTURI<sup>1</sup>, Nana KUCHAVA<sup>1</sup>  
Nanuli BAGDAVADZE<sup>1</sup>, Eteri GELAGUTASHVILI<sup>1</sup>, Marina V. FRONTASYEVA<sup>3\*</sup>  
Inga ZINICOVSCAIA<sup>3,4</sup>, Sergey S. PAVLOV<sup>3</sup> and Andrey Y. DMITRIEV<sup>3</sup>

## GOLD AND SILVER NANOPARTICLES IN *Spirulina platensis* BIOMASS FOR MEDICAL APPLICATION

### BIOMASA *Spirulina platensis* Z NANOCZĄSTKAMI ŻŁOTA I SREBRA DO ZASTOSOWAŃ MEDYCZNYCH

**Abstract:** The synthesis of gold and silver nanoparticles by the blue-green algae *Spirulina platensis* for medical purposes was studied. A complex of optical and analytical methods was used in order to characterize produced nanoparticles. It was shown that the extracellular formation of metal nanoparticles of spherical shape with sizes in the range between 8 and 40 nm (the average size of 20-30 nm) takes place. The characteristics of gold and silver nanoparticles in the *Spirulina* biomass were compared. The role of biosorption processes in the synthesis of nanoparticles was estimated by using equilibrium dialysis. A positive influence of sonication on the process of microbial synthesis and yield of nanoparticles were demonstrated. The neutron activation analysis and the atomic absorption spectrometry were applied for characterizing the dynamics of gold and silver nanoparticles formation in the *Spirulina platensis* biomass. The neutron activation analysis was used for studying the elemental content of the *Spirulina platensis* biomass.

**Keywords:** gold, silver, nanoparticles, *Spirulina platensis*, biotechnology, optical and analytical methods, ultrasound

## Introduction

The development of ecologically friendly nanotechnologies for production of new medical substances, including the nanoscale production, has recently become of considerable importance in expenditure of their biological and medical applications. Nanomaterials have unique physical and chemical properties, which can be used to overcome some limitations of traditional medicine [1]. Nanoparticles can be engineered in

<sup>1</sup> E. Andronikashvili Institute of Physics, I. Javakhishvili State University, 6 Tamarashvili Str., Tbilisi 0177, Georgia

<sup>2</sup> Iliia State University, 3/5 K. Cholokashvili Ave., Tbilisi 0162, Georgia

<sup>3</sup> Joint Institute for Nuclear Research, 6 Joliot-Curie Str., 1419890, Dubna, Russia

<sup>4</sup> The Institute of Chemistry of the ASM, 3 Academiei Str., 2028 Chisinau, Moldova

\*Corresponding author: marina@nf.jinr.ru

a way that allows them to be attracted to cells to facilitate earlier detection and direct treatment of some diseases.

A variety of inorganic nanoparticles with well-defined chemical composition, size, and morphology has been synthesized by using different microorganisms. Their applications in biology and medicine have been explored as well [2]. Metals are required for the proper sustenance and growth of all microorganisms. Some of these microorganisms have developed highly efficient metal-scavenging systems for capturing and concentrating specific metal ions from a solution; the other ones do not possess such active systems [3]. Bacterial surfaces are typically anionic and interact with metal cations. Gram-positive microbial walls consist of a variety of hetero- and homopolymers, which in combination can produce an electronegative charge density throughout the cell wall. Metal nanoparticles production takes place as extracellularly, as well as intracellularly.

Gold and silver nanoparticles represent a class of metallic nanoparticles with great potential for a variety of applications in medicine, such as oncology, cardiology, immunology, neurology, and endocrinology.

A variety of studies has shown that gold nanoparticles are promising as anticancer agents. Gold nanoparticles have good optical and chemical properties for use in the tumors infrared phototherapy; therefore, they can be used for earlier detection and treatment of different types of cancer. The optical effect of gold nanoparticles is associated with the collective excitation of conduction electrons and is localized in a broad region, from visible to infrared. It depends on the particle size, shape, and structure in laser therapy, gold nanoparticles injected in the body, are accumulated in a tumor. Subsequently, the tumor areas are illuminated with a near-infrared laser at wavelengths where light has its maximum depth of penetration in tissue. Gold nanoparticles are capable to specifically absorb this laser light, converting it into heat and selectively destroying the tumor tissue.

The activity of silver ions and silver-based compounds, including silver nanoparticles, is well known. Silver nanoparticles have unique optical, electrical, magnetic and thermal properties and are being incorporated into photo, biological and chemical sensors. Silver has long been used to exhibit a strong toxicity to a wide range of microorganisms. Many biomedical devices contain silver ions to inhibit bacterial action [6, 7].

The blue-green microalgae *Spirulina platensis* (*S. platensis*) is one of the most widely used microorganisms in the biotechnology of nutrition, pharmaceuticals, and medicine. It is the world's richest natural source of vegetable proteins, amino acids, vitamins, essential fatty acids, beta carotene, iron, and other biologically active beneficial substances. *Spirulina* is often used as a matrix for pharmaceuticals as well as a biologically active food additive for humans and animals [8-10]. Being a living organism, it accumulates essential elements (Se, I, Cr and others) and produces complexes easily assimilated by the human organism in sufficient quantity. It may be hypothesized that the biomass of *S. platensis* with gold and silver nanoparticles has great potential for medical applications. The synthesis of nanoparticles by *S. platensis* has been studied elsewhere [11, 12].

In our earlier investigations, *S. platensis* was used as a matrix for the development of new pharmaceutical substances [13-16]. The elemental content of the initial biomass of *Spirulina* was studied using the neutron activation analysis; it was shown that the concentrations of some toxic elements in the biomass of *S. platensis* do not exceed permissible levels [14].

The synthesis of silver and gold nanoparticles by the biomass of *S. platensis* was studied in [17] and [18], respectively. The present work is a continuation of these studies.

## Materials and methods

### Sample preparation

In all the experiments, the strain of *S. platensis* IPPAS B-256 from the A.K. Timiriyaev Institute for Plant Physiology of the Russian Academy of Sciences was used. The cultivation conditions for *S. platensis* cells in standard water-salt nutrient medium are described elsewhere [13, 14]. After 5-day cultivation, cells of *S. platensis* were separated from the culture broth by centrifugation (12,000 g) for 20 min, and then the biomass was washed twice with sterile distilled water. The harvested biomass (1 g) was resuspended in 250-ml Erlenmeyer flasks with 100 ml of  $10^{-3}$  M aqueous chloroauric acid (HAuCl<sub>4</sub>) solution for synthesis of gold nanoparticles and aqueous silver nitrate (AgNO<sub>3</sub>) solution for synthesis of silver nanoparticles. The resulting mixtures were again put into the shaker (200 g) at room temperature with pH 5-8 for different time periods (1 to 6 days).

### Methods

A complex of spectral and analytical methods was used to characterize gold and silver nanoparticles in the *S. platensis* biomass: ultraviolet-visible spectrometry (UV-Vis), X-ray diffraction (XRD), transmission electron microscopy (TEM), scanning electron microscopy (SEM) with energy-dispersive analysis of X-rays (EDAX), equilibrium dialysis, atomic absorption spectrometry (AAS), and neutron activation analysis (NAA).

For the UV-Vis spectral analysis and TEM, 5-ml samples of the suspension were taken at different time intervals. For SEM, XRD, AAS, and NAA, the bacterial cells in each case were harvested by centrifugation at 12,000 g for 20 min. The wet biomass was placed in an adsorption-condensation lyophilizer [19] and dried to constant weight.

The UV-visual spectra of samples were recorded by the Cintra-10 spectrophotometer (Australia). The XRD measurements of the *S. platensis* biomass were made at the Dron-2.0 diffractometer. TEM was performed using the JEOL SX-100 (Japan) equipment. SEM was carried out using the Quanta 3D FEG with the EDAX Genesis system. A flame AAS was carried out with the Beckman-495 spectrometer.

The elemental content of *S. platensis* samples was determined using NAA at the IBR-2 reactor of the Frank Laboratory of Neutron Physics (FLNP), JINR, Dubna, Russia. The concentrations of elements based on short-lived radionuclides were determined by 60-s irradiation under a thermal neutron fluency rate of approximately  $1.6 \times 10^{13}$  n cm<sup>-2</sup> s<sup>-1</sup>. Following the decays of 2 and 20 minutes, the samples were measured for 5 and 20 min, respectively. To determine long-lived isotopes, a cadmium-screened irradiation channel under a resonance neutron fluency rate of approximately  $3.31 \times 10^{12}$  n cm<sup>-2</sup> s<sup>-1</sup> was used. The samples were irradiated for 5 days, repacked and then measured twice following the decays of 4 and 20 days. The counting time varied from 30 min to 1.5 hours.

The gold content was determined with the 411.8-keV  $\gamma$  line of <sup>198</sup>Au and silver content with the 657.7-keV  $\gamma$  line of <sup>110m</sup>Ag.

The spectra of induced  $\gamma$  activity were processed using the Genie 2000, and concentrations were calculated by means of software developed at FLNP JINR [20].

## Results

The UV-Vis spectrometry was used for testing the biomass of *S. platensis* with gold and silver nanoparticles. Dose dependency of absorption versus chloroauric acid and silver nitrate concentrations within a range of  $10^{-2}$ - $10^{-4}$  M in the UV-Vis spectra by first was studied for *S. platensis*. The optimal concentration in both cases was near  $10^{-3}$  M. At a concentration of  $10^{-2}$  M, the sizes of nanoparticles were larger than 100 nm, and the peaks were not observed.

The UV-Vis spectra of absorbance at concentrations of  $10^{-3}$  M of gold and silver compounds and different reaction time are given in Figures 1a and 1b, respectively [17, 18]. In these figures, the peak intensity for nanoparticles of specific sizes increased as a function of the reaction time.

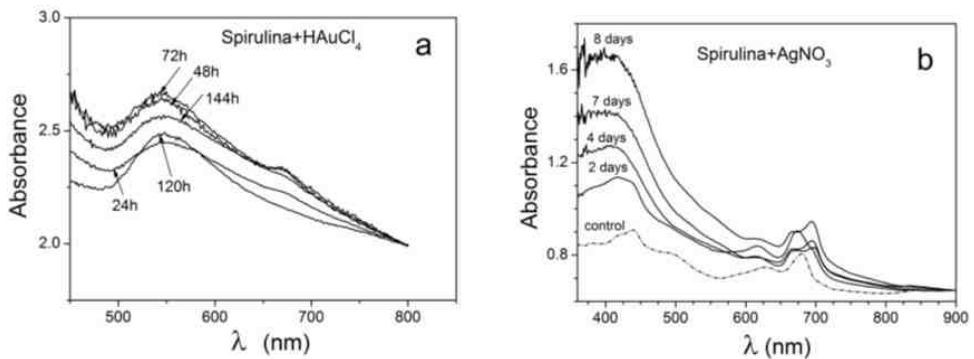


Fig. 1. UV-Vis spectra of absorbance of gold (a) and silver (b) nanoparticles for different reaction time

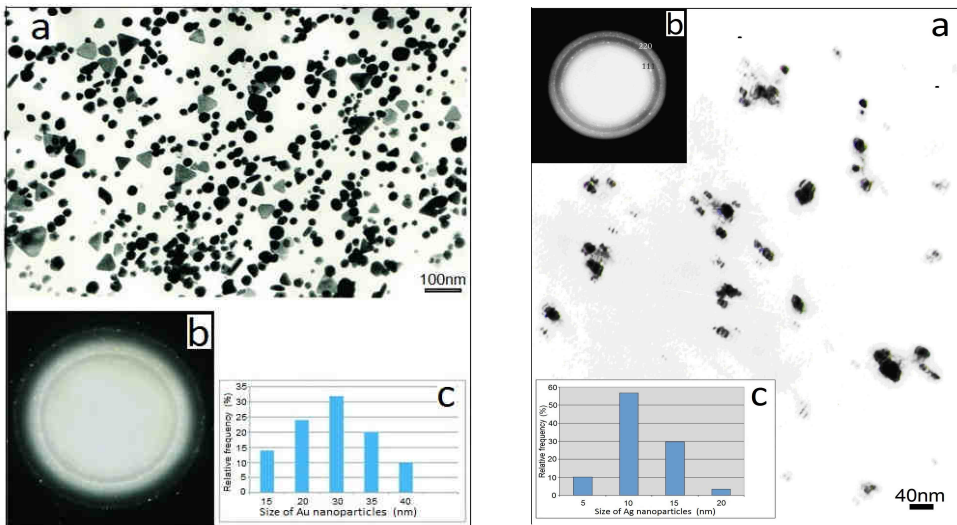


Fig. 2. TEM images of nanoparticles in *S. platensis* biomass (a), selected area diffractograms (b), and nanoparticle sizes distributions (c) for Au (left) and Ag (right), respectively

In the TEM, images for the *Spirulina* biomass with gold and silver nanoparticles of spherical and other shapes were observed. The diffraction patterns corresponded to the face-centered cubic (fcc) structure. Figure 2a shows a TEM image and a diffractogram of Au nanoparticles synthesized in the biomass of *S. platensis* treated by  $\text{HAuCl}_4$   $5 \cdot 10^{-3}$  M solution for 5 days. The particle size histogram for the studied sample shows that the sizes of gold nanoparticles varied within the range between 15 to 40 nm, with an average of 25-30 nm. Figure 2b shows the TEM image and a diffractogram of Ag nanoparticles synthesized in the biomass of *S. platensis* treated with  $\text{AgNO}_3$   $10^{-3}$  M solution for 5 days. The particle size histogram shows that the sizes of silver nanoparticles varied in the range between 5 to 20 nm, with an average of 10-15 nm.

The XRD data for gold and silver nanoparticles synthesized by *S. platensis* confirmed the presence of an fcc structure. For instance, Figure 3 shows the XRD pattern of gold nanoparticles synthesized by treating *S. platensis* with chloroauric acid aqueous  $10^{-3}$  M solution for 4 days. The diffraction patterns revealed an amorphous structure of nanoparticles. However, a number of Bragg reflections corresponding to the fcc structure of gold and silver were also seen in both cases, *ie*, four characteristic peaks (111), (200), (220), and (311).

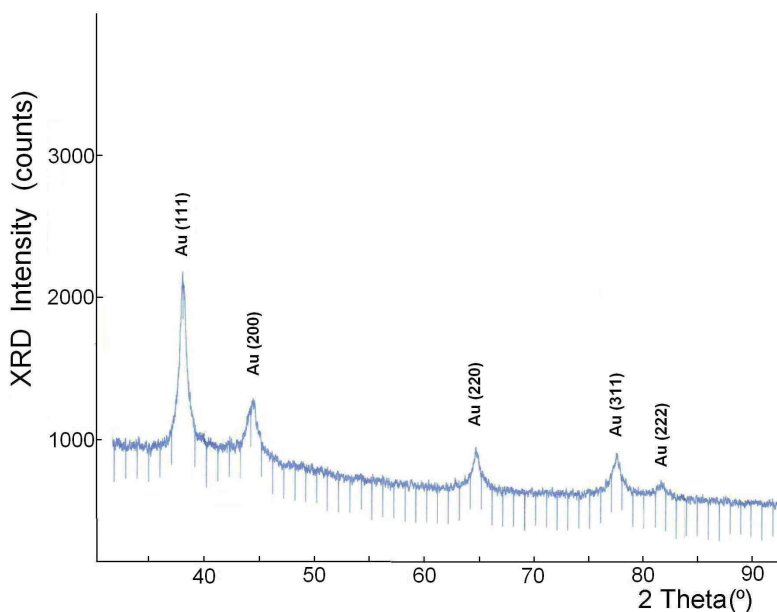


Fig. 3. XRD pattern of gold nanoparticles synthesized by treating *S. platensis* with chloroauric acid aqueous of  $10^{-3}$  M solution for 4 days

The Scherrer equation [21, 22] applicable to grains less than  $0.1 \mu\text{m}$  was used for an approximate assessment of the nanoparticle sizes based on broadening of one of interference peaks on the diffractogram (Fig. 3). The obtained results showed that at the  $\text{HAuCl}_4$  concentration of  $10^{-3}$  M,  $5 \cdot 10^{-3}$  M, and  $10^{-2}$  M, the size of gold nanoparticles

was  $\approx 14$ ,  $\approx 20$ , and  $\approx 100$  nm, respectively [18]. These results were in good agreement with those obtained by using the TEM image.

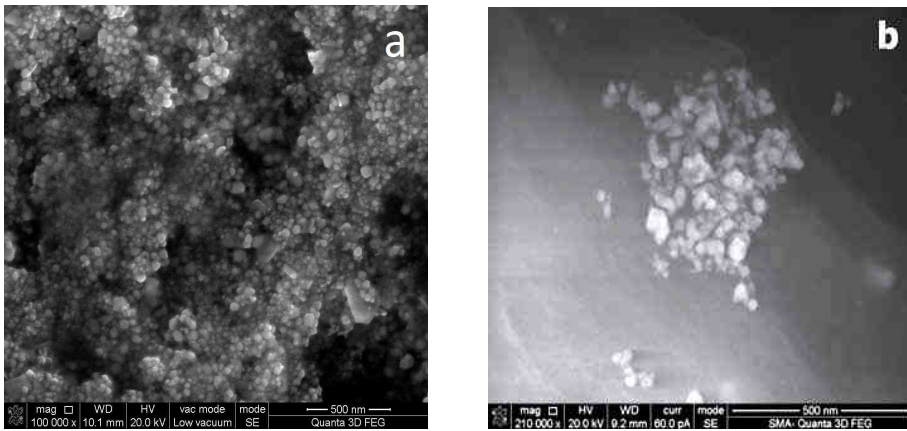


Fig. 4. SEM image of *S. platensis* cells with gold (a) and silver (b) nanoparticles

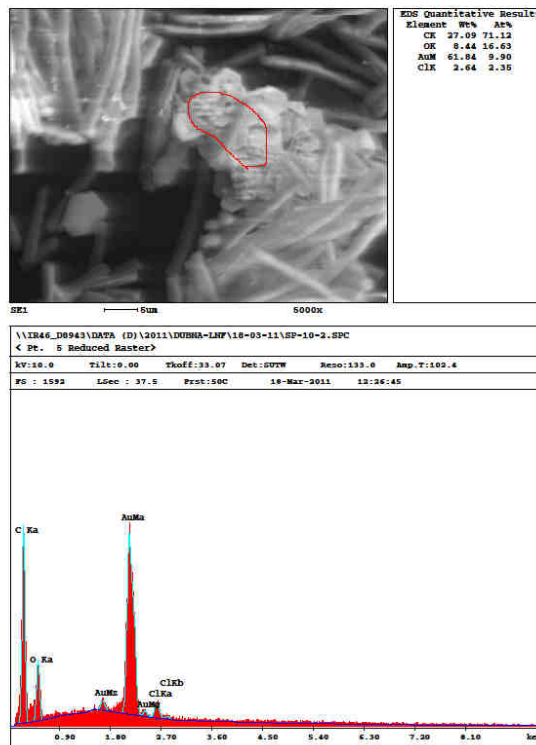


Fig. 5. EDAX spectra of gold nanoparticles in *S. platensis* cells

Figure 4a presents an example of a SEM image of *S. platensis* cells after their interaction with  $\text{HAuCl}_4$  at a concentration of  $5 \cdot 10^{-3} \text{ M}$  for 5 days. The image illustrates that most of the particles were spherical and did not create big agglomerates. Figure 4b shows an example of a relatively large agglomerate (27 nm) formation at the synthesis of silver nanoparticles by the *S. platensis* biomass treated with  $\text{AgNO}_3$  at a concentration of  $10^{-3} \text{ M}$  for 1 day.

The example of the EDAX X-ray spectra proved the presence of gold nanoparticles in *S. platensis* cells: three peaks of Au were observed (Fig. 5). Signals from C, O, and Cl atoms were also recorded. Their presence was likely due to the X-ray emissions from the proteins and enzymes that were present in the cell wall.

Two analytical methods - NAA and AAS - were used to study the growth dynamics of gold and silver total concentrations in the biomass of *S. platensis*. The obtained results showed that the dependence of metal concentrations on the interaction time of gold and silver compounds with the solution containing *Spirulina* cells were similar in all the studied cases. For example, see Figures 6a and b, where Au concentrations in *S. platensis* determined by NAA and AAS, respectively, are presented.

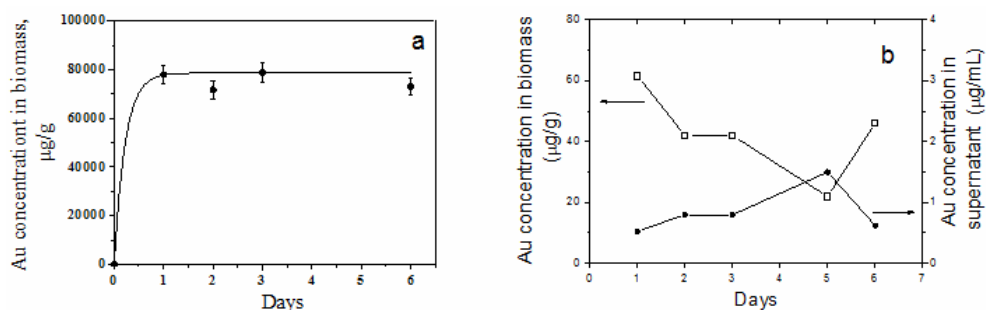


Fig. 6. Au concentrations in *S. platensis* determined by NAA (a) and the Au concentrations in *S. platensis* biomass and supernatant determined by AAS (b)

To study the biosorption process on *S. platensis* cells during nanoparticle production, the method of equilibrium dialysis and AAS were used. The concentration of metal sorbed by *Spirulina* in solution at equilibrium obeyed the Freundlich equation and suggested the presence of heterogeneous sorption sites on the cell surfaces [23].

The study of biosorption of Au by *Spirulina platensis* was carried out at various pH values. The experimental data were fitted to the Freundlich model, in which the capacity of the adsorbent and the equilibrium relationships between adsorbent and adsorbate are described by the Freundlich adsorption isotherms:

$$C_b = KC_t^{1/n}$$

where  $C_b$  is the concentration of the metal adsorbed,  $C_t$  is the equilibrium concentration of metal ions in a solution,  $K$  and  $n$  are empirical constants, which may be characterized as the biosorption constant and sorption capacity, respectively. In Figure 7, the biosorption isotherms of Au-*S. platensis* at various pH are presented.

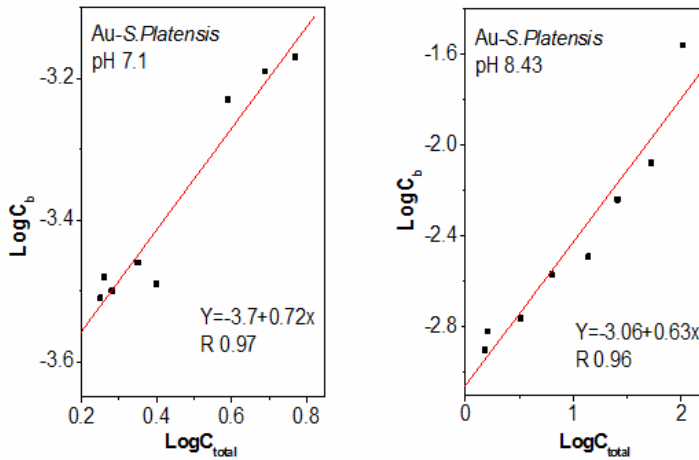


Fig. 7. Biosorption isotherms for Au - *Spirulina platensis* fitted using the Freundlich model at various pH

The process of biosorption in compliance with the Freundlich model showed its strong dependence on the surface properties of microbial cells. These results encouraged us to increase the total surface of *S. platensis* by reducing in size its fibers by sonicating the suspension with ultrasound to disrupt cell membranes. The experiment was carried out during the synthesis of gold nanoparticles. The concentration of  $\text{HAuCl}_4$  solution was  $10^{-3}$  M.

Following 10-minute ultrasound application at 35 kHz, *Spirulina* was comminuted into small fragments (0.5-1  $\mu\text{m}$ ), which was clearly visible by an optical microscope with x400 magnification. Accordingly, an increase in the total sorption surface was observed.

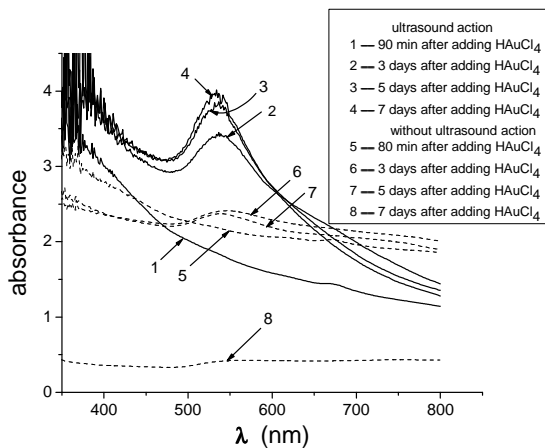


Fig. 8. Spectra of the gold nanoparticles obtained for *S. platensis* subjected to ultrasound (1, 2, 3, 4) and without subsection to ultrasound (5, 6, 7, 8)

Figure 8 shows the UV-Vis spectra of the *S. platensis* biomass with gold nanoparticles obtained through ultrasonic irradiation and without ultrasound influence. It emerged that the surface plasmon peak value at 530 nm in the case of ultrasound influence on *Spirulina* was about 4 times more intense than the one without subsection to ultrasound.

The size distribution of gold nanoparticles determined for this sample by using the TEM imaging is given in Figure 9. The average size of the gold nanoparticles decreased down to 16 nm.

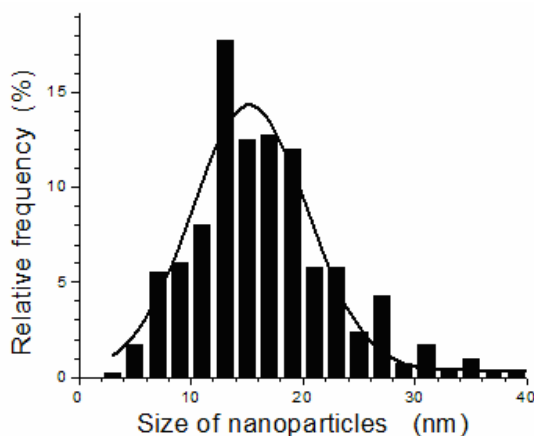


Fig. 9. Size distribution of the gold nanoparticles in *Spirulina* after subsection to ultrasound

NAA was also used to study multi-elemental content of *S. platensis* samples, taking into account the possible medical application of the obtained substances with Au and Ag nanoparticles.

## Discussion

As is known, absorption bands of surface plasmons in the UV-Vis absorption spectra depend on particle size and the dielectric constant of the medium and surface-adsorbed species. The gold surface plasmon resonance (SPR) peak at ~ 530 nm corresponded to aggregation in the solutions of gold nanoparticles, which were formed by gold ion reduction from Au(III) to Au (0) by biomolecules, proteins and enzymes on the surface of bacteria cells [18]. The spectra in silver case exhibited an absorption peak at 425 nm, which is typical of silver nanoparticles and corresponds to silver reduction from Ag(I) to Ag (0) [19]. The shape of plasmon resonance absorption bands depended on the particle morphology [24]. Single SPR bands were expected in the adsorption spectra of spherical isotropic nanoparticles.

At higher concentrations, the number of active objects on the surface of *Spirulina* cells that were involved in the synthesis was not sufficient for the reduction of metal ions [25]. Consequently, synthesis depended on the metal concentration as well as on the number of cells in solution. This differential response indicates the possibility of custom-designed nanoparticles by varying cell number and metal concentration in solution.

As could be seen from the comparison of the spectra for gold and silver nanoparticles in the *S. platensis* biomass, the surface plasmon gold peak at 530 nm was more separated than the silver peak at 425 nm. Such difference could be caused by dispersed sizes of the nanoparticles, dielectric properties of the medium, and the poor state of surface-adsorbed species on *S. platensis* cells due to the antibacterial properties of silver.

The results obtained by XRD clearly showed that the gold and silver nanoparticles formed by bacterial reduction of ions were crystalline in nature; moreover, they were generally produced extracellularly. The comparison of the XRD spectra for Au and Ag nanoparticles in the *Spirulina* biomass also showed that the peaks of Au were higher than those of Ag.

The data obtained by NAA and AAS analytical methods illustrated that on the first day the metal concentration increased rapidly; afterwards, it did not significantly change. During the “rapid” phase, the metal ions were mainly adsorbed on the surface of microorganisms by the biomolecular functional groups that can bind metal ions and are synthesized extracellularly. During the second (“slow”) phase, the metal ions were transported across the cell membrane into the cytoplasm and accumulated intracellularly.

The NAA multi-elemental results showed that the concentrations of some toxic elements (such as Hg, As, Cd, etc.) in the biomass under investigation did not exceed permissible levels [26]; moreover, it was revealed that the biomass of *S. platensis* containing gold and silver nanoparticles could be used for medical, pharmaceutical, and nutrition purposes.

## Conclusions

The results of the performed study showed that the blue-green algae *Spirulina platensis* effectively produced gold and silver nanoparticles by interacting with aqueous solutions of chloroauric acid ( $\text{HAuCl}_4$ ) and silver nitrate ( $\text{AgNO}_3$ ), respectively.

The gold and silver nanoparticles formed by algal biomass were shown/proved to be crystalline in nature and were produced mostly extracellularly. In general, they proved to have spherical shapes and sizes in the range of 5 to 40 nm. Total concentrations of gold and silver determined in the biomass showed that on the first day the metal ions were rapidly adsorbed mostly into the cell surface and then slowly transported into bacterial cells. The experiments carried out using a method of equilibrium dialysis confirmed the importance of surface processes in the synthesis of metal nanoparticles. The use of ultrasound for the sonicating *Spirulina* biomass increased the nanoparticles production yield.

The concentrations of some toxic elements in the *Spirulina platensis* biomass did not exceed permissible levels, and the obtained nanomaterials turned out to have great potential, especially for medicine and pharmacology.

The developed microbial methods of nanoparticle biosynthesis proved to be innovative, simple, non-toxic, and applicable to many branches of science and industry.

## Acknowledgements

The authors acknowledge the Ukrainian Science and Technology Centre (STCU) Grants # 4744 and # 5002.

## References

- [1] Salata OV. J Nanobiotechnol. 2004;2:1-6. DOI:10.1186/1477-3155-2-12.
- [2] Li X, Xu H, Chen ZS, Chen G. J Nanomat.2011;1-16. DOI:10.1155/2011/270974.
- [3] Beverige TJ. Int Rev Cytol. 1981;72:229-317.
- [4] Hirsch LR, Stafford RJ, Bankson JA, Sershen SR, Rivera B, Price RE, et al. Proc Natl Acad Sci USA. 2003;100:13549-135554. DOI:10.1073/pnas.2232479100.
- [5] Dykman LA, Khlebtsov NG. Acta Naturae. 2011;3:34-55. PMID:22649683.
- [6] Singh M, Singh S, Prasad S, Gambhir IS. Dig J Nanomater Bios. 2008;3:115-122.
- [7] Ahamed M, Alsali MS, Siddiqui MK. Clin Chim Acta. 2010;411:1841-1848. PubMed: 20719239.
- [8] Kim CJ, Jung YH, Oh HM. J Microbiol. 2007;45:122-127.
- [9] Belay A, Ota Y, Miyakawa K, Shimamatsu H. J Appl Phycol. 1993;5:235-241.
- [10] Doshi H, Ray A, Kothari IL. Biotechnol Bioeng. 2007;96:1051-1063. DOI 10.1002/bit.21190.
- [11] Sadowski Z. Biosynthesis and Application of Silver and Gold Nanoparticles. In: Pozo Perez D, editor. Silver nanoparticles. InTech; 2010. DOI: 10.5772/8508.
- [12] Govindaraju K, Basha SK, Kumar VG, Singaravelu G, J Mater Sci. 2008;43:5115-5122.
- [13] Mosulishvili LM, Belokobylsky AI, Kirkesali EI, Frontasyeva MV, Pavlov SS, Aksanova NG. J Neutron Res. 2007;15: 49-54. DOI: 10.1080/10238160601025138.
- [14] Mosulishvili LM, Frontasyeva MV, Pavlov SS, Belokobylsky AI, Kirkesali EI, Khizanishvili AI, et al. J Pharm Biomed Anal. 2002;30:87-97. PubMed PMID: 12151068.
- [15] Mosulishvili LM, Belokobylsky AI, Kirkesali EI, Frontasyeva MV, Pavlov SS. Method of production of chromium-containing pharmaceuticals based on blue-green algae *Spirulina platensis*. R. F. Patent No 2230560, June 11; 2002.
- [16] Mosulishvili LM, Belokobylsky AI, Khizanishvili AI, Kirkesali EI, Frontasyeva MV, Pavlov SS. Method of production of selenium-containing pharmaceuticals based on blue-green algae *Spirulina platensis*. R. F. Patent No 2209077, March 15; 2001.
- [17] Tsiakhashvili NY, Kirkesali EI, Pataraya DT, Gurielidze MA, Kalabegishvili TL, Gvarjaladze DN, et al. Adv Sci Lett. 2011;4:3408-3417.
- [18] Kalabegishvili T, Kirkesali E, Rcheulishvili A, Ginturi E, Murusidze I, Kuchava N, et al. Adv Sci Eng Med. 2013;5:30-36.
- [19] Mosulishvili LM, Nadareishvili VS, Kharabadze NE, Belokobylsky AI. Facility for Lyophilization of Biological Preparation. URSS Patent No 779765, Bul. 42; 1980.
- [20] Dmitriev AYU, Pavlov SS. Particles and Nuclei, Letters. 2013;10:58-64.
- [21] Cullity BD, Stock SR. Elements of X-Ray Diffraction. 3rd Ed. Prentice-Hall Inc.; 2001;167-171.
- [22] Jenkins R, Snyder RL. Introduction to X-ray Powder Diffractometry. John Wiley & Sons Inc.; 1996;89-91.
- [23] van Hullebusch ED, Zandvoort MH, Lens PNL. Rev Environ Sci Biotechnol. 2003;2:9-33.
- [24] Sosa IO, Noguez C, Barrera PG. J Phys Chem B. 2003;107:6269-6275.
- [25] Pimprikar S, Joshi SS, Kumar ARR, Zinjarde SS, Kulkarni SK. Colloid Surface B. 2009;74:309-316.
- [26] W.H.O. Elements in human nutrition and health, Geneva: WHO; 1996.

### BIOMASA *Spirulina platensis* Z NANOCZĄSTKAMI ŻŁOTA I SREBRA DO ZASTOSOWAŃ MEDYCZYNYCH

**Abstrakt:** Zbadano syntezę nanocząstek złota i srebra przez niebieskozielone glony *Spirulina platensis*, które są wykorzystywane do celów medycznych. Do scharakteryzowania wytworzonych nanocząstek zastosowano szereg metod optycznych i analitycznych. Wykazano, że zachodzi tworzenie pozakomórkowej, sferycznej nanocząstki o rozmiarach w zakresie od 8 do 40 nm (średnia wielkość 20-30 nm). Porównano charakterystyki nanocząstek złota i srebra wytworzonych w biomacie *Spiruliny*. Do oceny roli procesów biosorpcji w syntezie nanocząstek wykorzystano dializy równowagowe. Wykazano pozytywny wpływ ultradźwięków na procesy mikrobiologiczne i na wydajność syntezy nanocząstek. Do określenia dynamiki tworzenia nanocząsteczek złota i srebra w biomacie *Spirulina platensis* zastosowano neutronową analizę aktywacyjną i spektrometrię absorpcji atomowej. Stężenia pierwiastków w biomacie *Spirulina platensis* określono za pomocą neutronowej analizy aktywacyjnej.

**Słowa kluczowe:** złoto, srebro, nanocząstki, *Spirulina platensis*, biotechnologia, metody optyczne i analityczne, ultradźwięki